LHCb-CONF-2012-010
March 20, 2012

Search for the rare decays $B_s^0 \to \mu^+\mu^-\mu^+\mu^-$ and $B^0 \to \mu^+\mu^-\mu^+\mu^-$

The LHCb collaboration [1]

Abstract

A search for the decays $B_s^0 \to \mu^+\mu^-\mu^+\mu^-$ and $B^0 \to \mu^+\mu^-\mu^+\mu^-$ in a data sample of $1.0\,\text{fb}^{-1}$ collected with the LHCb detector in 2011 is discussed. In the SM, the non-resonant $B_s^0 \to \mu^+\mu^-\mu^+\mu^-$ branching fraction is expected to be $< 10^{-10}$. One signal candidate is observed in the B_d channel, and no signal candidates are observed in the B_s channel. These observed events are consistent with the expected backgrounds and upper limits on the branching fractions are set at $\mathcal{B}(B_s^0 \to \mu^+\mu^-\mu^+\mu^-) < 1.3 \times 10^{-8}$ and $\mathcal{B}(B^0 \to \mu^+\mu^-\mu^+\mu^-) < 5.4 \times 10^{-9}$ at 95% CL.

[1] Conference report prepared for the XLVIIth Recontres de Moriond session devoted to QCD and high energy interactions, La Thuile, 10-17 March 2012;
contact author: J. Albrecht, Johannes.Albrecht@cern.ch

1 Introduction

The decays of B mesons into final states with four muons are strongly suppressed in the Standard Model (SM). The largest contribution comes from $B_s \to J/\psi\phi$ with both the J/ψ and the ϕ mesons decaying into two muons. The corresponding branching fraction has been estimated to be $(2.3 \pm 0.9) \times 10^{-8}$ [1]. In the SM, the combined branching fraction of other possible B decay channels populating four muon final states is expected not to exceed 10^{-10} [2]. However, physics beyond the Standard Model may significantly enhance the $B \to \mu^+\mu^-\mu^+\mu^-$ branching fraction through flavour changing neutral currents mediated by new particles decaying into $\mu^+\mu^-$ pairs [3].

This document outlines the search for the rare decays $B_s^0 \to \mu^+\mu^-\mu^+\mu^-$ and $B^0 \to \mu^+\mu^-\mu^+\mu^-$. The data set for this analysis corresponds to $1.0\,\text{fb}^{-1}$ of pp collisions recorded with the LHCb detector in 2011 [4].

2 Event Selection

A cut-based selection was designed to maximise $\frac{S}{\sqrt{S+B}}$, where S is the number of events selected from a sample representing the signal, and B the number of background events in a mass sideband. The decay $B_s \to (\phi \to \mu\mu)(J/\psi \to \mu\mu)$ was used as a mode on which to tune the 4μ selections. Samples independent of the dataset used for the search were chosen for selection development and evaluation. Events with invariant mass in the range $4336 < M_{4\mu} < 6366$ MeV/c^2 were selected and the resulting dataset was split into two components:

- The resonant window: mass windows around the nominal J/ψ and ϕ invariant masses were used to select resonant candidates. The $M_{4\mu}$ mass window around the B_s^0 mass was used to count the number of $B_s^0 \to J/\psi\,\phi$ events, S, for the purpose of optimising the selection;
- The non-resonant window: The J/ψ and ϕ mass windows were vetoed for all opposite sign dimuon combinations.

	Mass Windows (MeV/c^2)	
	$B^0 \to \mu^+\mu^-\mu^+\mu^-$	$B_s^0 \to \mu^+\mu^-\mu^+\mu^-$
Optimisation mass sidebands	4336-4776 and 5966-6366	
Evaluation mass sidebands	4776-5220 and 5426-5966	
Blind mass window	5220-5340	5306-5426
Signal mass window	5240-5320	5326-5406

Table 1: The components of the non-resonant mass window for the B_d and B_s signal modes.

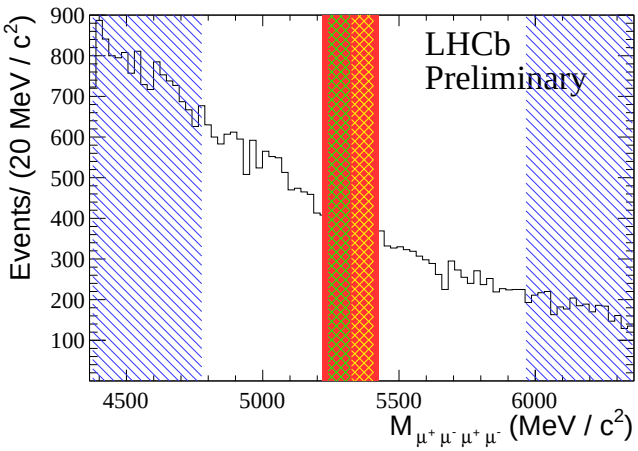

Figure 1: $M_{4\mu}$ invariant mass plot of the non-resonant window before selection. The blue regions indicate the optimisation mass sidebands. The red region indicates the blind mass window. The green (yellow) region indicates the B_d (B_s) signal mass window.

The non-resonant mass window was split into four components, shown in Table 1 and Figure 1. The optimisation mass sidebands were used to count the number of background events, B, when developing the selection. Data from the evaluation sidebands was used to perform an unbiased determination of the combinatorial background. The blinded mass window was excluded while developing the selection. After the analysis was fully finalized, it was unblinded and the number of events in the B_s and B_d signal windows were counted to extract their respective signal yields.

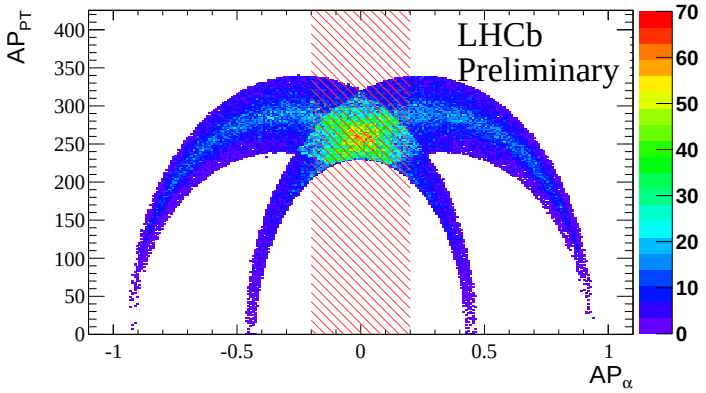

Figure 2: A plot of the variables AP_α against AP_{PT}, as described in the text. The red region indicates the $K \leftrightarrow \pi$ veto.

$B_q^0 \to \mu^+\mu^-\mu^+\mu^-$	
Selection	Criteria
B: χ^2_{IP}	< 9
B: vertex χ^2/DOF	< 6
μ: χ^2_{IP}	> 16
μ: $\mathrm{DLL}_{K-\pi}$	< 0
μ: $\mathrm{DLL}_{\mu-\pi}$	> 0
Veto $m_{J/\psi}$:	$m_{\mu\mu} < 3000\,\mathrm{MeV}/c^2$ or $m_{\mu\mu} > 3200\,\mathrm{MeV}/c^2$
Veto m_ϕ:	$m_{\mu\mu} < 950\,\mathrm{MeV}/c^2$ or $m_{\mu\mu} > 1090\,\mathrm{MeV}/c^2$
$B_d \to K^* J/\psi$	
Selection	Criteria
B_d: χ^2_{IP}	< 9
B_d: vertex χ^2/DOF	< 6
μ,K,π: χ^2_{IP}	> 16
μ: $\mathrm{DLL}_{K-\pi}$	< 0
μ: $\mathrm{DLL}_{\mu-\pi}$	> 0
Veto m_{B+}:	$5220 > m_{J/\psi K^+} > 5340\,\mathrm{MeV}/c^2$
Veto m_ϕ:	$950 > m_{K^+\pi^-_{PID=K}} > 1090\,\mathrm{MeV}/c^2$
$K \leftrightarrow \pi$ veto :	$-0.2 > AP_\alpha > 0.2$
K^*:	$826 < M_{K\pi} < 966\,\mathrm{MeV}/c^2$
J/ψ :	$3040 < m_{\mu\mu} < 3140\,\mathrm{MeV}/c^2$

Table 2: Selection criteria for the signal and control channels.

Table 2 shows the selection criteria for the signal and control channel, $B_d \to K^* J/\psi$ which is used to measure the branching fraction. For both channels cuts were applied on: the quality of the B decay vertex, $\chi^2_{/DOF}$; for the final state muons, the difference in the log-likelihood of the particle being assigned a muon (kaon) hypothesis or a pion hypothesis, $\mathrm{DLL}_{\mu-\pi}$ and $\mathrm{DLL}_{K-\pi}$; and the consistency of the B to originate from the primary vertex and of the final state particles to originate from a secondary vertex, χ^2_{IP}. Events were required to have been triggered by the main LHCb muon and dimuon triggers. For the control channel the background decay modes of $B^+ \to J/\psi K^+$ and $B \to K^*\phi$ were suppressed, by excluding candidates around the ϕ and B^+ mass, for the respective invariant mass combinations of $J/\psi K^+$ and $K^+\pi^-_{PID=K}$, where the pion is assigned a kaon mass hypothesis. The $M_{K\pi}$ and $M_{\mu\mu}$ invariant masses were required to be close to the nominal M_{K^*} and $M_{J/\psi}$ masses respectively.

Figure 2 shows a 2D plot of the variables $AP_\alpha = \frac{P_{l\mathbf{K}} - P_{l\boldsymbol{\pi}}}{P_{l\mathbf{K}} + P_{l\boldsymbol{\pi}}}$ against AP_{PT} for control channel data, where $P_{l\mathbf{K}}$ ($P_{l\boldsymbol{\pi}}$) is the longitudinal momentum of the K (π) with respect to the K^* direction in the laboratory frame and AP_{PT} is the transverse momentum of the pion with respect to the K^* momentum. The two arcs seen in the plot originate from the K^* and $\overline{K^*}$ respectively. In the region where the arcs overlap, each K^* decay product can be assigned with both pion and kaon mass hypotheses, creating duplicate events. A cut is applied on AP_α to remove these events.

Table 3 shows a full list of potential non-resonant peaking backgrounds that were considered for the analysis. These are given in the full B mass range. The expected yields in the signal region are found to be negligible.

Mode	Branching fraction	Branching fraction (including MisID)	Expected yield
$B_d \to (K^* \to K\pi)\,\mu^+\mu^-$	1.1×10^{-6}	3.3×10^{-10}	0.16
$B_s \to (\phi \to K^+K^-)\,\mu^+\mu^-$	7.6×10^{-7}	2.3×10^{-10}	0.11
$B_d \to K^+\pi^-\pi^+\pi^-$	$< 2.3 \times 10^{-4}$	$< 2.1 \times 10^{-11}$	< 0.01
$B_d \to (\rho^0 \to \pi^+\pi^-)\,\mu^+\mu^-$	$\sim 10^{-8}$ (est)	$\sim 10^{-12}$	< 0.01
$B_d \to (J/\psi \to \mu^+\mu^-)\,\pi^+\pi^-$	2.7×10^{-6}	8.2×10^{-10}	0.002
$B_d \to (J/\psi \to \mu^+\mu^-)\,(K^* \to K^+\pi^-)$	5.3×10^{-5}	1.2×10^{-9}	0.14
$B_s \to (J/\psi \to \mu^+\mu^-)\,(K^* \to K^+\pi^-)$	3.2×10^{-6}	0.7×10^{-10}	0.004
$B_s \to (J/\psi \to \mu^+\mu^-)\,(f^0(980) \to \pi^+\pi^-)$	7.6×10^{-6}	2.3×10^{-9}	0.007
$B_d \to (\psi(2S) \to \mu^+\mu^-)\,(K^* \to K^+\pi^-)$	3.1×10^{-6}	9.3×10^{-10}	0.44

Table 3: Expectations for non-resonant peaking backgrounds. No limits for $B_d \to (\rho^0 \to \pi^+\pi^-)\,\mu^+\mu^-$ have been published, so an expected branching fraction is used instead. Note that the yields given cover the complete B mass range. For a combined $K \to \mu$ and $\pi \to \mu$ mass hypothesis exchange, the fraction of events in the signal region is 3%.

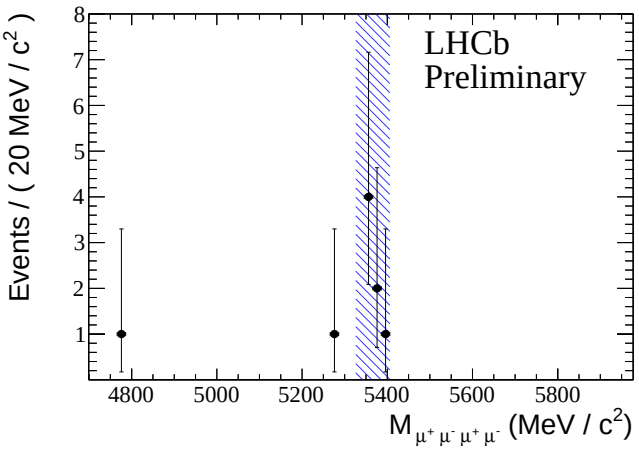

Figure 3: $M_{4\mu}$ invariant mass plot of the resonant window after selection, the blue region indicates the B_s signal window.

Figure 3 shows the resonant window after the selection. In the resonant window seven $B_s^0 \to J/\psi\,\phi$ candidates are observed. In the non-resonant window six background candidates remain in the evaluation sideband. These six events were fitted with a single exponential, yielding an estimate for the background expected in the B_s (B_d) signal mass window of $0.38^{+0.23}_{-0.17}$ ($0.30^{+0.22}_{-0.20}$). Fitting a linear function to the background events gave consistent results.

3 Measurement of the branching fraction

The branching fraction was measured by normalising to the control channel $B^0_d \to J/\psi(\to \mu^+\mu^-)K^{*0}(\to K^+\pi^-)$. The same kinematic and PID selection criteria were applied to this control channel and to the signal channel.

Figure 4 shows the $M_{K\pi\mu\mu}$ distribution after the selection. Both the B_d and B_s mass peaks were fitted with double gaussian and radiative tail probability density functions, along with a single exponential background pdf [5]. The B_d mass peak contains 35476 $\pm$ 286 events.

The signal and control channels have different reconstruction and selection efficiencies which arise from differences in their kinematic distributions. To account for this, the branching fraction is computed using the relative efficiency of reconstructing signal and control channel events. This relative efficiency is taken from simulated events. The decay products of the signal were simulated according to a phase space distribution. The kinematic distributions of the simulated events were found to be in good agreement with data. The total efficiencies of the signal and control channels were found to be 0.359 $\pm$ 0.003% and 0.273 $\pm$ 0.003% respectively.

Systematic errors were calculated for effects which result from discrepancies between simulation and data. The following effects were considered: the trigger; the calculation of $\mathrm{DLL}_{\mu-\pi}$ and $\mathrm{DLL}_{K-\pi}$; the efficiency of reconstructing tracks; and the χ^2_{IP} distributions of the particles. The combined uncertainty was found to by 5.9%. This uncertainty was accounted for in the limit setting procedure described below.

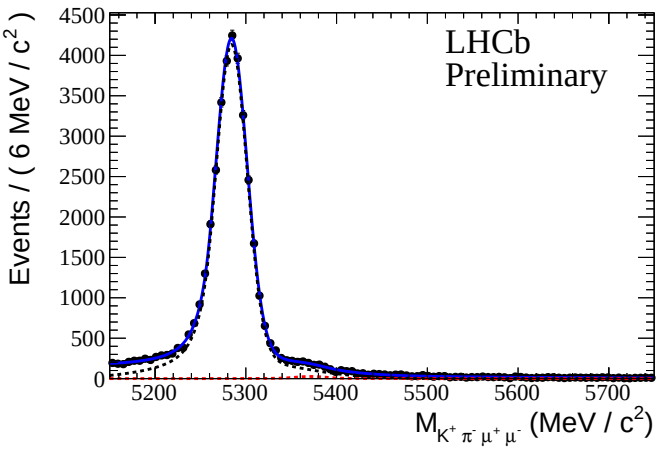

Figure 4: The invariant mass distribution of $K^+\pi^-\mu^+\mu^-$ candidates after the application of the selection criteria. The PDF for the B^0 and B^0_s signal distributions are shown in black and red respectively.

4 Results

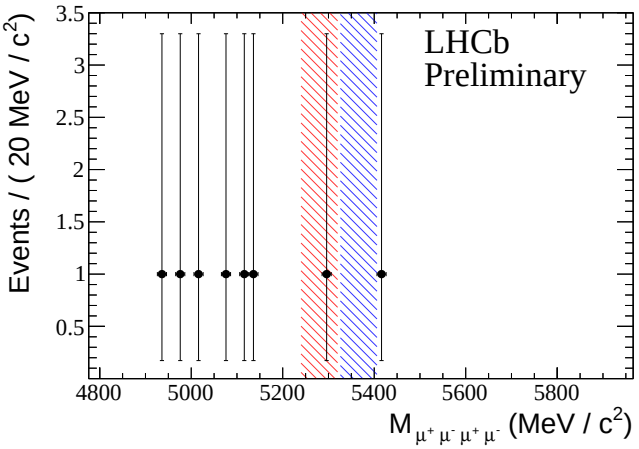

Figure 5: $M_{4\mu}$ invariant mass plot of the non-resonant window after unblinding, the blue (red) region indicates the B_s (B_d) signal window.

Figure 5 shows the unblinded $M_{4\mu}$ mass range of the non-resonant window. One event is observed in the B_d signal window and no events are observed in the B_s window. These observations are consistent with the expected background yield. The compatibility of the observed distribution of events in all bins with the distribution expected for a given branching fraction hypothesis was computed using the CL_s method
[6, 7]. The CL_s method provides three estimators: CL_{s+b}, a measure of the compatibility of the observed distribution with the signal and background hypotheses, CL_b, a measure of the compatibility with the background-only hypothesis, and $CL_s = CL_{s+b}/CL_b$, which yields the final confidence level CL$= 1 - CL_s$.

The corresponding 95% CL BR limits are: $\mathcal{B}(B_s^0 \to \mu^+\mu^-\mu^+\mu^-) < 1.3 \times 10^{-8}$ and $\mathcal{B}(B^0 \to \mu^+\mu^-\mu^+\mu^-) < 5.4 \times 10^{-9}$.

References

[1] Particle Data Group, K. Nakamura et al., *Review of particle physics*, *J. Phys.* **G37** (2010) 075021.

[2] D. Melikhov and N. Nikitin, Phys. Rev. D **70**, 114028, (2004);.

[3] S. Demidov and D. Gorbunov, *Flavor violating processes with sgoldstino pair production*, `arXiv:1112.5230`.

[4] LHCb collaboration, A. A. Alves Jr. et al., *The LHCb detector at the LHC*, *JINST* **3** (2008) S08005.

[5] D. Martinez Santos, J. J. Saborido Silva, P. Alvarez Cartelle, A. Dosil Suarez, and A. Yanez Santamaria, *Measurement of the $B_s \to J\psi K^*$ branching ratio in LHCb*, . LHCb-CONF-2011-025.

[6] A. Read, Presentation of Search Results: The CL_s Technique, J. Phys. **G28** (2002) 2693.

[7] T. Junk, Confidence Level Computation for Combining Searches with Small Statistics, Nucl. Instrum. Meth. **A434** (1999) 435, hep-ex/9902006.